

CrossMark  
click for updatesCite this: *RSC Adv.*, 2017, 7, 5583

# Corrosion of carbon steel induced by a microbial-enhanced oil recovery bacterium *Pseudomonas* sp. SWP-4

Guihong Lan,<sup>\*ab</sup> Chao Chen,<sup>b</sup> Yongqiang Liu,<sup>c</sup> Yinchun Lu,<sup>b</sup> Jiao Du,<sup>b</sup> Sha Tao<sup>b</sup> and Shihong Zhang<sup>b</sup>

*Pseudomonas* sp. SWP-4 has been proved to enhance oil recovery effectively. However, corrosion to oil wells or pipes needs to be evaluated when SWP-4 is used. This study investigated the corrosion behavior of carbon steel induced by SWP-4. Results indicated that a mild effect on corrosion occurred in medium with SWP-4. Electrochemical parameters ( $E_{\text{corr}}$ ,  $I_{\text{corr}}$ , and  $R_{\text{ct}}$ ) suggested that SWP-4 promoted the corrosion in the exponential phase in the fastest growth time. Surface morphologies and corrosion products were detected by using scanning electron microscopy and energy dispersive X-ray spectroscopy. Moreover, this study proved that oil-cell-free fermentation broth could inhibit the corrosion and the growth of sulphate-reducing bacteria and saprophytic bacteria.

Received 13th October 2016  
Accepted 25th November 2016

DOI: 10.1039/c6ra25154d

www.rsc.org/advances

## 1. Introduction

Microbial Enhanced Oil Recovery (MEOR) methods, making use of microbial activities and metabolic byproducts to decrease the viscosity and to improve the fluidity of crude oil,<sup>1</sup> have been investigated successfully in laboratory and field conditions, especially in low temperature oilfield reservoirs.<sup>2–5</sup> Genus *Pseudomonas* as a high-efficiency crude oil degrader degrading *n*-alkanes<sup>6,7</sup> and producing rhamnolipid to reduce surface tension both have been considered to be used in the MEOR process.<sup>8</sup>

Microbiologically influenced corrosion (MIC) is of considerable concerns in the oil, gas and marine industries, which results in high corrosion costs. MIC happens due to the bacteria activity and bacterial metabolites in the oil field's water injection systems. To date, most of the studies about *Pseudomonas* species in the corrosion process of mild steel, stainless steel and aluminum alloys were involved in marine environments. These *Pseudomonas* strains have also been demonstrated to accelerate and lead to the occurrence of the corrosion of metals and stainless steels.<sup>11–16</sup> For instance, Franklin *et al.*<sup>11</sup> found that *Pseudomonas* sp. attached on the carbon steel surface may inhibit repassivation which could make pits continue to grow. Hamzah *et al.*<sup>12</sup> and Morales *et al.*<sup>13</sup> found that microbial

deposits could induce the occurrence of pitting corrosion and metabolites production may thin the external passive film layer during the presence of *Pseudomonas aeruginosa*. Moradi *et al.*<sup>14</sup> suggested that the adhesion of *Pseudomonas* sp. and the biofilm with Cl, K and Na could induce localized corrosion of 2205 duplex stainless steel. Pedersen *et al.*<sup>15</sup> suggested that *Pseudomonas* sp. promoted passivity breakdown by excreting organic acids resulting in an increase in the corrosion rate of metals. Busalmen *et al.*<sup>16</sup> manifested that the enhancement in corrosion rate was due to the cathodic reduction by the catalase excreted by the genus *Pseudomonas*. In addition, Beech *et al.* demonstrated that the metal cations binding by extra-cellular polymeric substances (EPS) could facilitate the ionization of AISI 316 stainless steel surface, thus resulting in thinning the protective layers and changing the electrochemical nature of the metal surface.<sup>17–19</sup> In recent years, the metal ion chelating properties of bacterial EPS have been considered as an important role in microbiologically influenced corrosion (MIC) of metals.<sup>20,21</sup> Several investigations have been carried out to verify the corrosive effect of EPS on metal.<sup>21,22</sup> The nature of the composition of EPS excreted by bacteria has been extensively investigated to determine which functional groups caused the acceleration of corrosion.<sup>15,17,19–21,23</sup>

To inhibit corrosion, a large amount of works have been investigated in the adsorption of chemical surfactants. For the past few years, biosurfactants were also investigated as environment-friendly corrosion inhibitors to pre-treatment the surface of steel.<sup>24,25</sup> However, surface-active compounds had not been elaborated further in these literatures.

Sulphate-reducing bacteria (SRB) as the prominent groups of microorganisms causing corrosion of steels and stainless steels have been extensively investigated.<sup>26–29</sup> Biocide has widely been

<sup>\*</sup>Key Laboratory of Oil & Gas Applied Chemistry of Sichuan Province, Southwest Petroleum University, No. 8 Xindu Avenue, Xindu District, Chengdu 610500, PR China. E-mail: guihonglan416@sina.com; Fax: +86 02883037306; Tel: +86 02883037306

<sup>b</sup>College of Chemistry and Chemical Engineering, Southwest Petroleum University, Chengdu 610500, PR China

<sup>c</sup>Faculty of Engineering and the Environment, University of Southampton, Southampton SO17 1BJ, UK

used to control the corrosion of different metals and alloys by microorganisms. Additionally, rhamnolipid as a promising biosurfactant has been investigated to have the antibacterial capability in the areas of food and healthcare.<sup>30–34</sup> Its surface-active compound has also been tested for very good anti-adhesive properties to prevent contamination of stainless steel surfaces by different pathogenic bacteria.<sup>31</sup> However, there is hardly a literature reporting about the effects of environmental biosurfactant (rhamnolipid) on the most harmful bacteria corroding the steel on oilfield such as sulphate-reducing bacteria (SRB) and saprophytic bacteria (TGB).

In the previous study,<sup>9</sup> we isolated a strain *Pseudomonas* sp. SWP-4 which was able to degrade waste cooking oil (WCO) to produce rhamnolipid with low critical micelle concentration and high surface activities. Moreover, we have found that the addition of WCO had positive effects on heavy crude oil degradation and MEOR process.<sup>10</sup> The MEOR treatments are always conducted through injecting bacteria and nutrients with the normal water flooding operation or fermentation broth to enhance additional oil recovery. To apply *Pseudomonas* sp. SWP-4 in the process further, it is necessary to study the corrosivity of the bacteria towards materials used in seawater injection systems. The present study aims to gain a further understanding on the influence of *Pseudomonas* sp. SWP-4 and the oil-cell-free fermentation broth respectively on the corrosion behavior of carbon steel as a function of time in a mineral salts medium using mass loss measurement, electrochemical techniques, scanning electron microscopy (SEM) and energy dispersive X-ray spectra (EDS) analysis. In addition, the antibacterial capability of the oil-cell-free fermentation broth on the SRB and TGB are also implemented.

## 2. Materials and methods

### 2.1. Metal sample preparation

The carbon steel Q235 used in this study contains 99.22% Fe, 0.37% Mn, 0.20% Si, 0.17% C, 0.03% S, 0.01% P and other trace elements. Sheet specimens of carbon steel with dimensions of 50 × 25 × 2 mm were used for SEM and EDS analysis. Metallic specimens used as working electrode had an exposed area of 1 cm<sup>2</sup> in the electrochemical study. The electrical connection was made through copper wire protected with epoxy resin. Prior to the experiments, specimens were successively ground using a series of 240, 400, 800, 1000, 1200 and 2000 grits silicon carbide papers. The polished specimens were subsequently rinsed with deionized (DI) water thrice, then degreased with acetone, sterilized with UV light and immersion in 70% ethanol for 1 h, and finally dried in a laminar flow cabinet.<sup>15</sup> The newly-prepared specimens were immediately used in the corrosion experiments.

### 2.2. Medium and inoculum cultivation

*Pseudomonas* sp. SWP-4 isolated as described in previous study<sup>10</sup> was stored in glycerol freezer stock at −40 °C in a refrigerator. Before each experiment, one Cryo tube was thawed at 35 °C for 15 min. The preculture was incubated in Luria–Bertani (LB)

medium: 10 g L<sup>−1</sup> tryptone, 5 g L<sup>−1</sup> yeast extract and 5 g L<sup>−1</sup> NaCl, while mineral salts medium (MSM) for corrosion experiments contained the following components: 4 g L<sup>−1</sup> NaNO<sub>3</sub>, 5 g L<sup>−1</sup> NaCl, 1 g L<sup>−1</sup> KH<sub>2</sub>PO<sub>4</sub>, 1 g L<sup>−1</sup> K<sub>2</sub>HPO<sub>4</sub>, 0.2 g L<sup>−1</sup> MgSO<sub>4</sub> · 7H<sub>2</sub>O, 0.2 g L<sup>−1</sup> FeSO<sub>4</sub> · 7H<sub>2</sub>O, 0.2 g L<sup>−1</sup> CaCl<sub>2</sub>, 20 g L<sup>−1</sup> WCO. Each medium was autoclaved at 121 °C for 20 min before use.

### 2.3. Cultivation of *Pseudomonas* sp. SWP-4 at static condition

In previous work, we have studied the dynamic growth curve of *Pseudomonas* sp. SWP-4.<sup>9</sup> In this study, the static growth curve of *Pseudomonas* sp. SWP-4 was studied with MSM at static condition. The optical density at a wavelength of 600 nm (OD<sub>600</sub>) of the oil-free broth (diluted by six times with the sterile mineral salts medium) was measured to indicate bacteria densities every 4 h during the culture period of 420 h with an ultraviolet spectrophotometer (V-1800, Kyoto, Japan). Meanwhile, the pH of the oil-free broth was measured every 12 h in the whole culture period with Youke pH meter (PHS-3E, Shanghai, China). Biosurfactant concentration was analyzed with anthrone–sulfuric acid colorimetric method,<sup>35,36</sup> and the rhamnose value was calculated from the standard curves prepared with L-rhamnose (10–90 mg L<sup>−1</sup>). The concentration of rhamnolipid was calculated by multiplying rhamnose value with 3.4, obtained from the correlation of pure rhamnolipid.<sup>9,37</sup>

### 2.4. Mineral salts oil-cell-free fermentation broth

These experiments were performed in 250 mL flasks containing 100 mL MSM inoculated with *Pseudomonas* sp. SWP-4 2 mL at 35 °C, 150 rpm for 3 days. To acquire the oil-cell-free fermentation broth, the supernatant containing the biosurfactant was separated from the cells and residual oil by centrifuging for 15 min at 3000 rpm. The oil-cell-free broth was stored at −4 °C for the following experiments.

### 2.5. Weight loss experiments

Carbon steel specimens with dimensions of 50 mm × 20 mm × 5 mm were used for the weight loss experiments. Weight loss of carbon steel specimens was monitored to evaluate corrosion.

To investigate the corrosion effect of carbon steel specimens in *Pseudomonas* sp. SWP-4 culture and the oil-cell-free broth, two sets of experiments were designed. In the first set of experiment, the influence of *Pseudomonas* sp. SWP-4 on the corrosion of carbon steel was investigated. The specimens were immersed in the MSM with and without *Pseudomonas* sp. SWP-4 for 12, 48, 96, 168, 216, 348, and 420 hours. In the second set of experiments, carbon steel specimens were exposed in mineral salts oil-cell-free fermentation broth got sterile deionised water was used as the control for 168, 336, 504, and 672 hours.

All the experiments were conducted in triplicates and the average was taken as the final result. Prior to the experiment, carbon steel specimens were weighed by a high-precision electronic analytical balance recorded as *m*<sub>0</sub>. After the experiment, the corrosion products and the biofilm grew on the surface of carbon steel specimens during the experiments period were removed following the procedure in the ASTM G1. Specimens



were weighed again and recorded as  $m_1$ , and the corrosion rate was calculated through the weight loss method.<sup>38</sup> The corrosion rate was calculated as follows:

$$v = 8.76 \times \frac{m_0 - m_1}{At\rho} \quad (1)$$

where  $v$  is the average corrosion rate, mm per year;  $m_0$  is the sample initial weight, g;  $m_1$  is the weight of the sample after removing the corrosion products and biofilm, g;  $A$  is the area of the specimen,  $\text{m}^2$ ;  $t$  is the exposure time, year;  $\rho$  is the density of the metal,  $\text{g cm}^{-3}$ .

## 2.6. Electrochemical studies

To measure the Tafel plots and the electrochemical impedance spectroscopy, electrochemical tests were performed in a conventional three-electrode glass corrosion cell with a capacity of 250 mL. An Ag/AgCl electrode connected to the working electrode (WE) through a Luggin's capillary was used as the reference electrode and a carbon electrode was used as the counter electrode (CE). All electrochemical tests were conducted using a computer-controlled system CHI650E (Shanghai Chenhua Instrument Company, China). Each electrochemical test was performed at a steady open circuit potential (OCP),  $E_{\text{OCP}}$ .

**2.6.1. Tafel polarization measurements.** The Tafel polarization curves were recorded at a scan rate of  $1 \text{ mV s}^{-1}$  within the range of  $-250$  to  $250 \text{ mV}$  versus the open circuit potential to determine the corrosion current density ( $i_{\text{corr}}$ ).

**2.6.2. Electrochemical impedance spectroscopy measurements.** The electrochemical impedance spectroscopy (EIS) was performed at a steady OCP and at an alternating current amplitude of  $10 \text{ mV}$  sine wave at frequencies ranging from  $10 \text{ kHz}$  to  $1 \text{ Hz}$ ; Zview software was used for EIS data analysis.

## 2.7. Surface topography analysis with SEM-EDS

The bacteria-colonized specimens underwent fixation and dehydration according to the procedures reported in literature before SEM and EDS analysis.<sup>39</sup> To assess the corrosion damage of specimens under the biofilms, ultrasonic treatment was used to remove biofilm. The specimens were immersed in a beaker with  $100 \text{ mL}$   $0.1 \text{ M}$  EDTA solution,<sup>40,41</sup> and, then, ultrasonicated for  $15 \text{ min}$  in a sonication bath with a frequency of  $40\text{--}50 \text{ kHz}$  to remove the corrosion products and the biofilms. The prepared specimens were then sputter-coated with gold/palladium, and subsequently detected with a scanning electron microscope and a energy dispersive X-ray spectra (JEOL JSM-7500F model & X-MAX50). The imaging sites for SEM were typically chosen on the specimen surface to be representative of the entire surface of the carbon steel specimens.

## 2.8. Evaluation of antibacterial effects

To mitigate the corrosion of carbon steel by harmful bacteria through reducing the quantities of them, the antibacterial effects of oil-cell-free fermentation broth were examined separately on SRB and TGB, and the concentrations of rhamnolipid in the broths were  $32 \mu\text{g mL}^{-1}$ ,  $96 \mu\text{g mL}^{-1}$ ,  $160 \mu\text{g mL}^{-1}$ ,  $320 \mu\text{g mL}^{-1}$ , and  $640 \mu\text{g mL}^{-1}$ , respectively. The bacteria were all

incubated at  $35^\circ\text{C}$  for  $24 \text{ h}$ , and then the most probable number (MPN) method was used to assess the quantities of bacteria.<sup>42</sup>

# 3. Results and discussion

## 3.1. Growth curve of *Pseudomonas* sp. SWP-4

The growth curve of *Pseudomonas* sp. SWP-4 under the static cultivation at  $30^\circ\text{C}$  was presented in Fig. 1. It can be seen that the growth curve of *Pseudomonas* sp. SWP-4 followed the traditional bacterial growth, i.e. lag phase, exponential phase, stationary phase and death phase. Before  $36 \text{ h}$ , the bacteria were at lag phase; during  $36\text{--}120 \text{ h}$ , it went into exponential phase, the number of active bacteria increased rapidly. It was found that rhamnolipid production accelerated in the exponential phase. In the death phase, although active bacterial concentration decreased significantly, rhamnolipid concentration remained at similar level as steady phase.

## 3.2. Corrosion of carbon steel in sterile medium and *Pseudomonas* sp. SWP-4 inoculated medium based on weight loss method

Fig. 2 shows dependence of the corrosion rate of specimens over the time during the corrosion process lasting for  $420 \text{ h}$  exposed in sterile medium and medium containing bacterium. In both cases, differences could be seen between samples exposed to sterile medium and medium containing bacterium. The corrosion rates of the steel specimens without and with *Pseudomonas* sp. SWP-4 calculated through the eqn (1) are shown in Fig. 2 respectively. During the first  $12 \text{ h}$ , the corrosion rates in sterile medium was  $0.2566 \text{ mm per year}$  a bit more than that in medium containing *Pseudomonas* sp. SWP-4,  $0.1961 \text{ mm per year}$ . However, during the first  $96 \text{ h}$ , the corrosion rates of the carbon steel specimens with *Pseudomonas* sp. SWP-4 showed a little more than that without *Pseudomonas* sp. SWP-4. After specimens immersed for  $420 \text{ h}$ , these data confirmed that when bacterium was added into the medium, the corrosion rate  $0.0136 \text{ mm per year}$  was approaching to without bacterium,

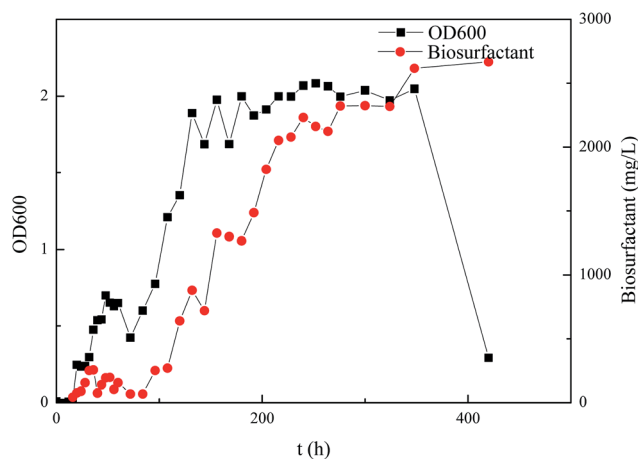


Fig. 1 Growth curve of *Pseudomonas* sp. SWP-4 and rhamnolipid concentration curves.



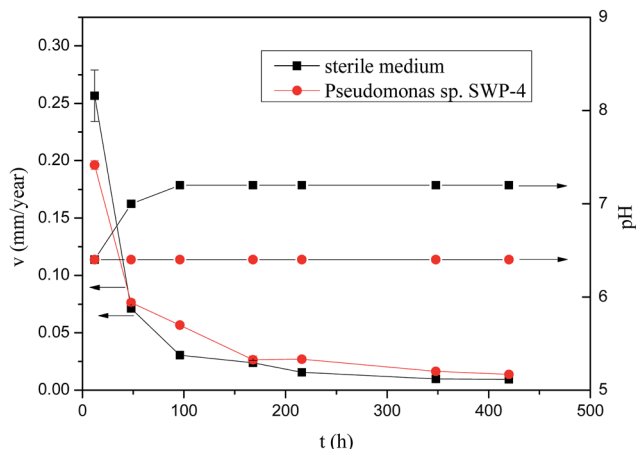


Fig. 2 Time dependence of corrosion rate of carbon steel and pH in sterile medium and medium containing *Pseudomonas* sp. SWP-4.

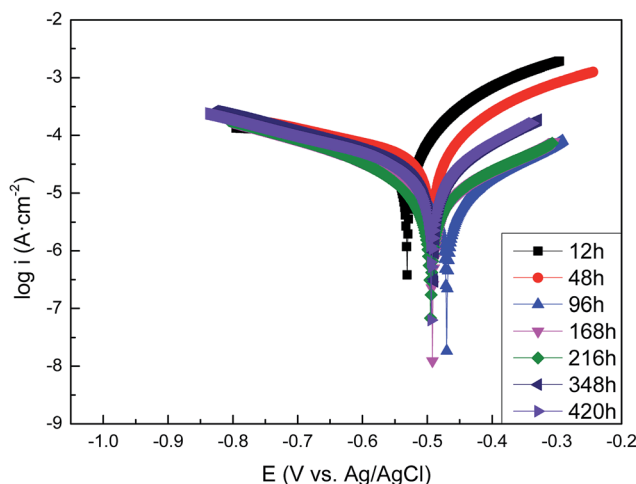


Fig. 3 Tafel plots of the carbon steel specimens in the sterile medium after different exposure periods: 12 h, 48 h, 96 h, 168 h, 216 h, 348 h, 420 h.

0.00935 mm per year, which meant *Pseudomonas* sp. SWP-4 influenced carbon steel efficiently and caused slight corrosion. It was quite different from the severely corrosive bacteria, *Pseudomonas aeruginosa*, reported by E. Hamzah,<sup>12</sup> with the corrosion rate of more than 0.1 mm per year. The pH values showed in Fig. 2. After inoculated with *Pseudomonas* sp. SWP-4, it increased to 7.2.

### 3.3. Corrosion of carbon steel in sterile medium and *Pseudomonas* sp. SWP-4 inoculated medium based on electrochemical measurements

**3.3.1. The polarization curves of carbon steel in sterile and *Pseudomonas* sp. SWP-4 inoculated media.** The polarization curves of the carbon steel after exposure to the sterile medium and the medium containing *Pseudomonas* sp. SWP-4 for different periods are shown in Fig. 3 and 4, respectively. The data of the electrochemical corrosion parameters such as the

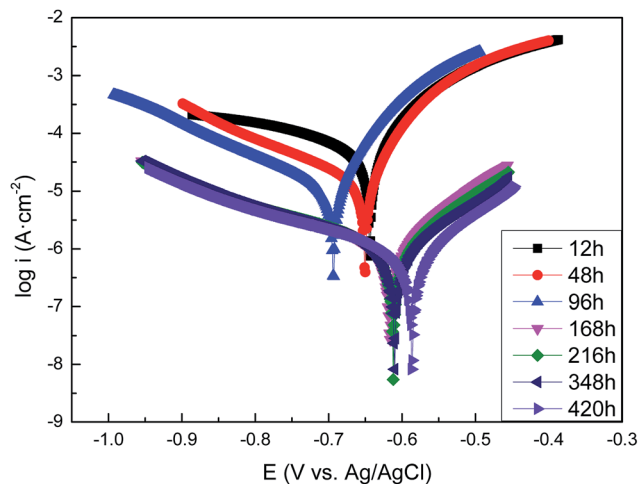


Fig. 4 Tafel plots of the carbon steel specimens in the *Pseudomonas* sp. SWP-4 inoculated medium after different exposure periods: 12 h, 48 h, 96 h, 168 h, 216 h, 348 h, 420 h.

corrosion potentials ( $E_{\text{ocp}}$ ), the Tafel slope (anodic slope  $\beta_a$  and cathodic slope  $\beta_c$ ), and corrosion current densities ( $i_{\text{corr}}$ ) are further analyzed with the extrapolation of the polarization and listed in Tables 1 and 2. At the beginning of the experiments, the  $E_{\text{corr}}$  and  $i_{\text{corr}}$  value of *Pseudomonas* sp. SWP-4-colonized carbon steel electrode were slightly more positive than the steel specimens in sterile medium, indicating that the bacterium induced an increase in the corrosion rate of carbon steel and its metabolites. In comparison with carbon steel in sterile medium for 420 h, the  $E_{\text{corr}}$  of the carbon steel underwent a negative shift of about 93 mV by the effect of the *Pseudomonas* sp. SWP-4 bacterium.

It is clearly seen from Fig. 3 that corrosion current densities,  $i_{\text{corr}}$ , decreased with exposure periods in the sterile medium, suggesting a decrease in the corrosion rate of the carbon steel with time owing to the formation of the protective oxide film. This was in good agreement with the results that the corrosion potential,  $E_{\text{corr}}$ , shifted from  $-0.531$  to  $-0.490$  V (vs. Ag/AgCl) after 420 h immersion.

For the exposure to the medium containing *Pseudomonas* sp. SWP-4, it was observed that, corrosion potential shifted from  $-0.644$  V to  $-0.694$  V (vs. Ag/AgCl) from 12 h to 96 h, corresponding to exponential phase of bacteria growth. In addition, the corrosion current densities,  $i_{\text{corr}}$ , decreased more slowly than that without *Pseudomonas* sp. SWP-4, which implied that bacteria may increase the corrosion rate in the exponential phase. Regarding to polarization curves, the cathodic branch in the MSM was attributed to the dissolved oxygen reduction; whereas, in the presence of *Pseudomonas* sp. SWP-4, the bacteria consumed the oxygen in the solution during the first 96 h, as a result, cathodic branch decreasing from  $-315$  to  $-187$  mV  $\text{dec}^{-1}$  refers to water reduction and hydrogen production. While the decrease in anodic branch from  $104$  to  $81$  mV  $\text{dec}^{-1}$  indicates that electron transfer became easier from the anodic site after the formation of the biofilm. After the exponential phase, it was found that  $i_{\text{corr}}$  reduced dramatically from  $11.96$  to  $0.95$





**Table 1** Tafel analysis of polarization curves of the carbon steel in the sterile medium after different exposure time

<i>T</i> (h)	<i>E</i> <sub>OCF</sub> (V vs. Ag/AgCl)	<i>I</i> <sub>corr</sub> (μA)	<i>i</i> <sub>corr</sub> (μA cm <sup>-2</sup> )	β <sub>a</sub> (mV dec <sup>-1</sup> )	β <sub>c</sub> (mV dec <sup>-1</sup> )
12	-0.531	57.62	57.62	119	-300
48	-0.493	58.30	58.30	134	-342
96	-0.47	8.125	8.125	160	-161
168	-0.492	10.46	10.46	170	-163
216	-0.495	7.543	7.543	173	-163
348	-0.49	24.48	24.48	149	-358
420	-0.494	23.14	23.14	150	-239

**Table 2** Tafel analysis of polarization curves of the carbon steel in the *Pseudomonas* sp. SWP-4 inoculated medium after different exposure periods

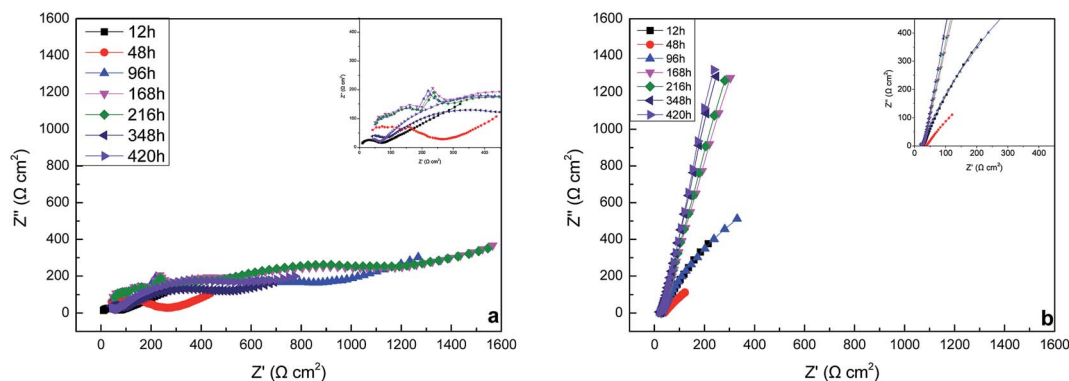
<i>T</i> (h)	<i>E</i> <sub>OCF</sub> (V vs. Ag/AgCl)	<i>I</i> <sub>corr</sub> (μA)	<i>i</i> <sub>corr</sub> (μA cm <sup>-2</sup> )	β <sub>a</sub> (mV dec <sup>-1</sup> )	β <sub>c</sub> (mV dec <sup>-1</sup> )
12	-0.644	68.51	68.51	104	-315
48	-0.650	23.16	23.16	87	-197
96	-0.694	16.22	16.22	81	-184
168	-0.616	1.336	1.336	107	-243
216	-0.612	1.286	1.286	116	-245
348	-0.612	1.174	1.174	123	-236
420	-0.587	0.950	0.950	118	-251

μA cm<sup>-2</sup> which was smaller than the value without *Pseudomonas* sp. SWP-4. It was speculated that this was probably caused by the inhibiting effect of the biosurfactant produced by *Pseudomonas* sp. SWP-4. It was different from the *Pseudomonas* investigated by S. J. Yuan.<sup>23</sup> The anodic Tafel slopes and cathodic Tafel slopes both increased, which supposed that the surface products made electron transfer became more difficult from the anodic site after the biosurfactant absorbed on the surface.

**3.3.2. The EIS of carbon steel in the sterile and *Pseudomonas* sp. SWP-4 inoculated medium.** EIS was conducted to illuminate the adhesion mechanism of *Pseudomonas* sp. SWP-4 to specimen surfaces, which was a complicated process affected by various physicochemical properties such as bacterial cells, metabolites and substratum surfaces.<sup>43</sup>

Fig. 5a, 6a and 7a respectively shows typical Nyquist and Bode plots determined for carbon steel in sterile medium at

different immersion periods. Fig. 5a shows Nyquist plots including a capacitive loop at high to medium frequencies and a straight line (Warburg impedance) at low frequencies. The presence of Warburg impedance reflects cathodic diffusion of dissolved oxygen from bulk solution to carbon steel electrode surface. The impedance value increased with exposure time because passive layers were formed on the metal surface. To describe the impedance response of corrosion in sterile medium, we proposed a similar circuit with two similar circuit, one relaxation-time constant for before 96 h (Fig. 8a) and two relaxation time constants after 96 h (Fig. 8b). In the circuit, *R*<sub>s</sub> is the resistance of solution, *R*<sub>b</sub> is pore resistance and *R*<sub>ct</sub> is the resistance of charge transfer, CPE<sub>b</sub> is the Constant Phase Element (CPE) parameter for the inhomogeneous layer, CPE<sub>dl</sub> is parameter for the electrical double layer and *C* is parameter for the double layer, *W* is parameter for the Warburg impedance.

**Fig. 5** Nyquist plots of the specimens in the sterile medium (a) and medium containing *Pseudomonas* sp. SWP-4 (b) after different exposure periods: 12 h, 48 h, 96 h, 168 h, 216 h, 348 h, 420 h.

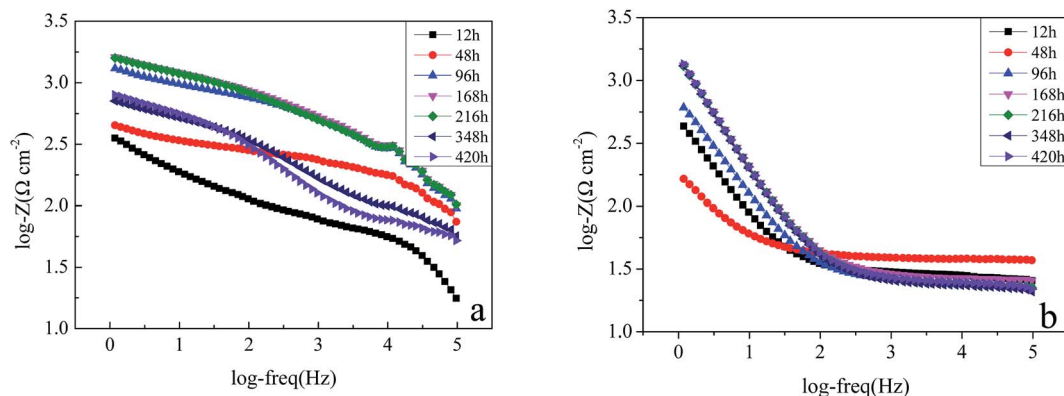


Fig. 6 Magnitude Bode plots of the specimens in the sterile medium (a) and medium containing *Pseudomonas* sp. SWP-4 (b) after different exposure periods: 12 h, 48 h, 96 h, 168 h, 216 h, 348 h, 420 h.

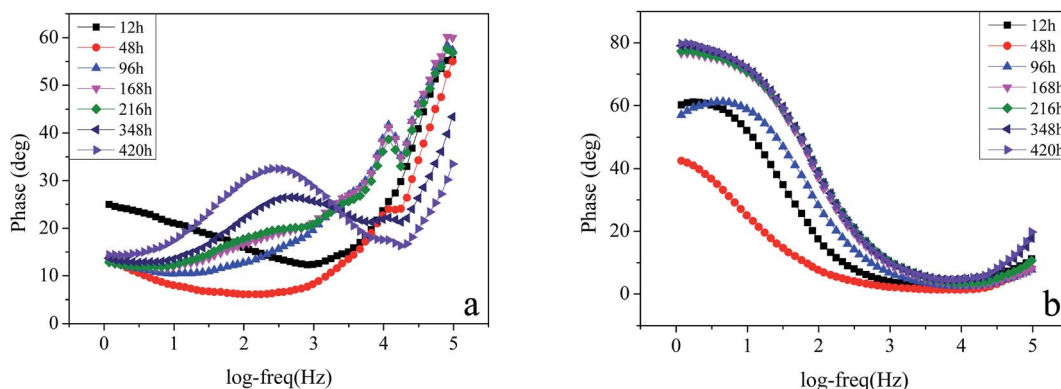


Fig. 7 Phase Bode plots of the specimens (a) in the sterile medium and medium containing *Pseudomonas* sp. SWP-4 (b) after different exposure periods: 12 h, 48 h, 96 h, 168 h, 216 h, 348 h, 420 h.

The second time constant represented the formation of a corrosion product and oxide layer on a metal surface.<sup>44</sup>

Nyquist and Bode plots for carbon steel in medium with SWP-4 at different immersion periods are illustrated in Fig. 5b, 6b and 7b. Before 96 h (including 96 h), since bacterial metabolism was very active, the physical and chemical

characteristics of medium containing bacteria were changeable due to the production of metabolites. The diameters of impedance loops in the Nyquist plots (Fig. 5b) decreased with time before 96 h, implying an accelerated corrosion of the carbon steel specimens. When bacteria attached to specimens (for 96 h), Nyquist plots was fitted with a two-time constant

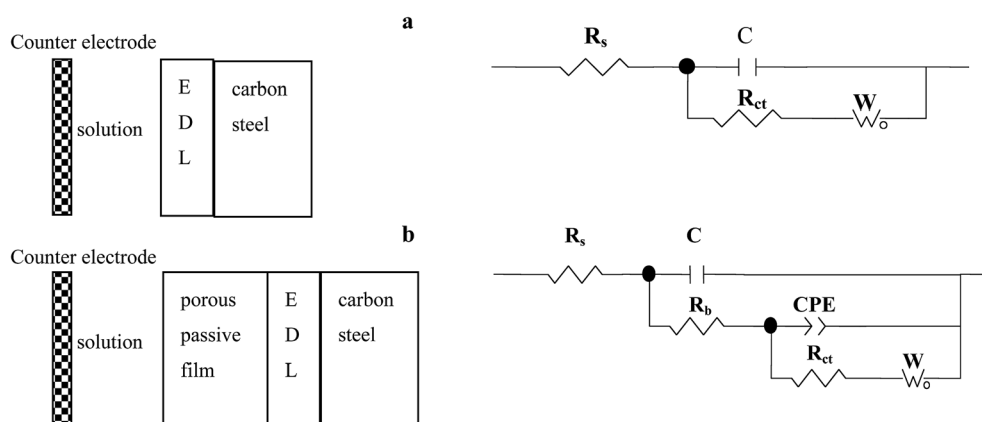


Fig. 8 Two physical models and the corresponding equivalent circuits used for fitting the impedance spectra of the specimens in the sterile medium. Equivalent circuits: (a) and (b).



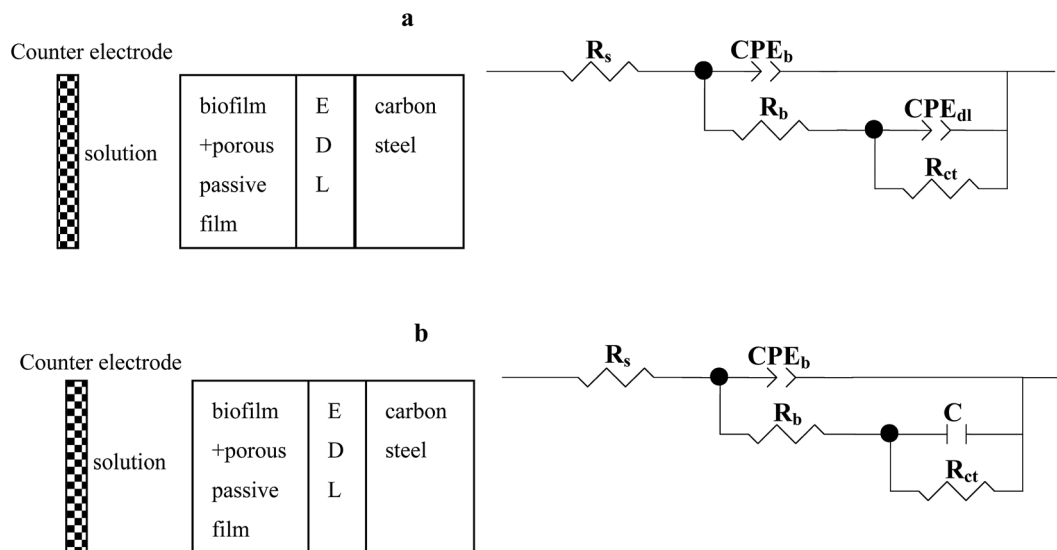


Fig. 9 Two physical models and the corresponding equivalent circuits used for fitting the impedance spectra of the specimens in the *Pseudomonas* sp. SWP-4-incubated medium. Equivalent circuits: (a) and (b).

Table 3 Fitting parameters of impedance spectra of specimens in the sterile medium after different exposure time

T/h	$R_s/\Omega\text{ cm}^{-2}$	$C/\mu\text{F cm}^{-2}$	$R_p/\Omega\text{ cm}^{-2}$	$\text{CPE-T}/\mu\Omega^{-1}\text{ s}^n\text{ cm}^{-2}$	CPE-P	$R_{ct}/\Omega\text{ cm}^{-2}$	$W_0\text{-R}/\Omega\text{ cm}^{-2}$	$W_0\text{-T}/\Omega^{-1}\text{ s}^n\text{ cm}^{-2}$	$W_0\text{-P}$	$\chi^2$
12	6.004	$9.52 \times 10^{-2}$				27.79	59.59	$1.26 \times 10^{-3}$	0.1700	0.0013
48	44.75	$3.99 \times 10^{-2}$				59.46	495.1	4.56	0.1300	0.0039
96	33.32	$2.46 \times 10^{-2}$	206.80	14.6	0.55803	545.00	9.345	$3.52 \times 10^{-7}$	0.1606	0.0053
168	28.97	$2.13 \times 10^{-2}$	196.20	41.2	0.45212	1072.0	6.983	$1.55 \times 10^{-6}$	0.1920	0.0049
216	37.80	$2.34 \times 10^{-2}$	208.00	44.1	0.47078	1103.0	4.858	$1.22 \times 10^{-6}$	0.1982	0.0045
348	46.06	$2.48 \times 10^{-2}$	235.20	35.0	0.49822	1209.0	24.96	$7.85 \times 10^{-5}$	0.1954	0.0045
420	41.12	$2.68 \times 10^{-2}$	163.20	37.8	0.55816	940.60	27.7	$2.05 \times 10^{-4}$	0.2036	0.0022

equivalent circuit showed in Fig. 9a and the results were listed in Table 4. A constant phase element (CPE) and capacitance were used due to the microscopic roughness of a surface.<sup>34–37</sup> Hence, corrosive biofilm formation initially increased, leading to decreased impedance value. Subsequently, corrosion impedance increased from 96 h. From 96 h to 216 h, another two-time constant circuit shown in Fig. 9b was used to analyze the impedance spectra and it was found that  $\text{CPE}_b\text{-T}$  and  $\text{CPE}_{dl}\text{-T}$  increased to  $60\ \mu\Omega^{-1}\text{ s}^n\text{ cm}^{-2}$  and  $70\ \mu\Omega^{-1}\text{ s}^n\text{ cm}^{-2}$ , respectively. The accumulation of rhamnolipid over the time increased  $R_{ct}$ . For 348 h and 420 h,  $C$  decreased to a stable value *i.e.*  $23\ \mu\text{F cm}^{-2}$ . The high concentration of rhamnolipid at this time increased  $R_{ct}$ , and thus decreased corrosion rate. The values of Chi-square  $\chi^2$  were all around  $10^{-3}$ , exhibiting the goodness of the equivalent circuit fits, as listed in Tables 3 and 4.

### 3.4. Corrosion of carbon steel in sterile medium and *Pseudomonas* sp. SWP-4 inoculated medium based on SEM micrographs and EDS spectrum

SEM micrographs and EDS spectrum to determine microbiologically influenced metal corrosion are used to observe the

microbial adhesion and the formation of the porous biofilm.<sup>21,23</sup> Fig. 10a shows that the surfaces of carbon steel exposed in sterile MSM for 420 h was covered by a corrosive oxide layer with large craters. Fig. 10b shows carbon steel surface after immersion in the medium with the presence of *Pseudomonas* sp. SWP-4 surfaces extensively covered with a thick biofilm layer, while Fig. 10c and e shows the intact biofilm-covered adhesion zones on carbon steel surface following compact bacterial exposure. EDS was used to obtain elemental information from corrosion products of typical areas on the surface of the carbon steel. The EDS analysis showed that oxide percentage of the specimens surface immersed in the sterile medium was 54.15% whereas the specimens immersed in the medium containing bacterium was 43.48%. It also showed that high amounts of Na, Mg, K, Ca as metabolic by-products (Table 5), which were ascribed to the halophilic characteristic. As a result, *Pseudomonas* sp. SWP-4 caused a reduction in the oxide percentage due to aerobic respiration. The elemental information from the corrosion products on the specimens surfaces was shown in Table 5. The results were in agreement with the previous study,<sup>15</sup> microbial adhesion and the consequent biofilm formation resulted in metal ion and chloride ion accumulation and induced corrosion.

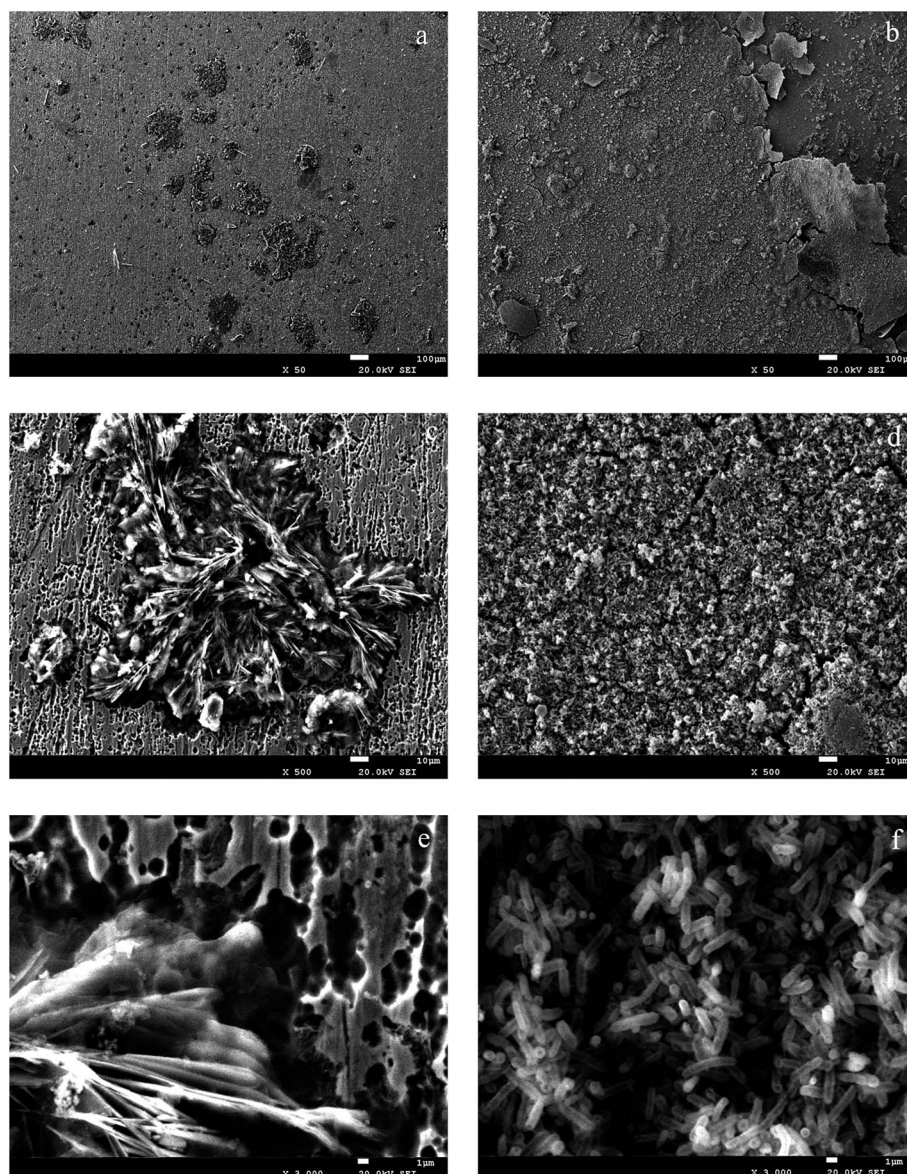


**Table 4** Fitting parameters of impedance spectra of specimens in the medium innovated *Pseudomonas* sp. SWP-4 after different exposure time

$t/h$	$R_s/\Omega\text{ cm}^{-2}$	$CPE_b\text{-T}/\mu\Omega^{-1}\text{ s}^n\text{ cm}^{-2}$	$CPE_b\text{-P}$	$R_p/\Omega\text{ cm}^{-2}$	$C/\mu\text{F}$	$CPE_{dl}\text{-T}/\mu\Omega^{-1}\text{ s}^n\text{ cm}^{-2}$	$CPE_{dl}\text{-P}$	$R_{ct}/\Omega\text{ cm}^{-2}$	$\chi^2$
12	27.86	440	0.7253	13.46	68.8			3226	0.0035
48	38.05	1414	0.697	79.5	159			448.2	0.0053
96	24.22	299	0.7602	25.5	26.1			2666.00	0.0019
168	26.2	60.8	0.8747	12.16		73.3	0.87169	$1.52 \times 10^5$	0.0016
216	23.32	57.3	0.8739	11.83		79.7	0.87036	$4.73 \times 10^5$	0.0026
348	23.13	110	0.8491	40.87	23.2			$1.51 \times 10^{11}$	0.0089
420	24.6	105	0.8566	45.05	22.9			$2.90 \times 10^{12}$	0.0072

Fig. 11a illustrates the surface of the carbon steel immersed in the sterile medium after corrosion products were removed, which suggested that anions like chloride in the MSM that probably accelerated the corrosion rate. Fig. 11b shows the

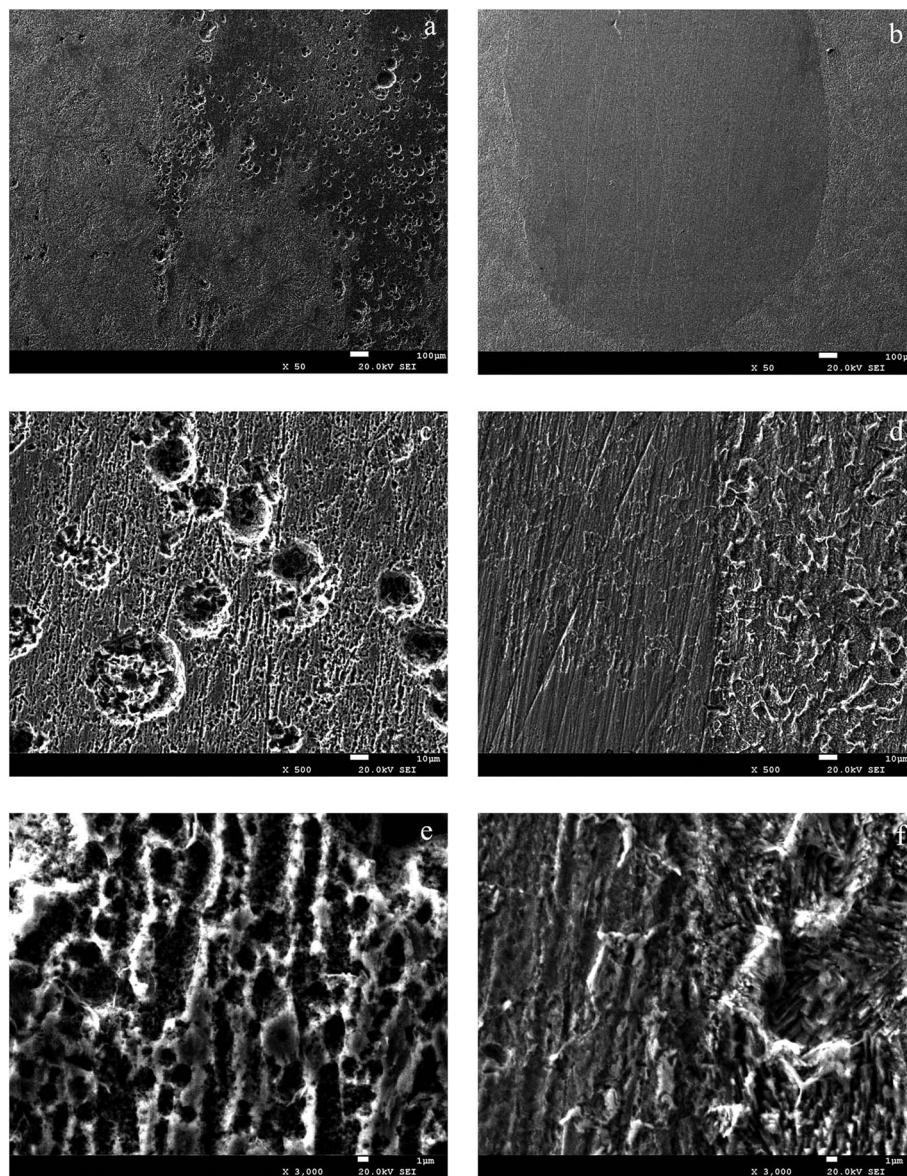
surface of the carbon steel corrosion immersed in the medium containing *Pseudomonas* sp. SWP-4 after corrosion products were removed. It clearly showed that the surface attached by porous biofilm and corrosion products was tougher than other

**Fig. 10** SEM images of products-attached and bacteria-colonized specimens after 420 h: (a), (c) and (e) (sterile medium); (b), (d) and (f) (medium with bacteria).



**Table 5** EDS spectrum of carbon steel surfaces exposed to sterile and containing bacteria medium

	C/%	O/%	Na/%	Mg/%	P/%	K/%	Ca/%	Fe/%
Sterile medium	30.45	54.15	0.27	0.26	5.15	0.07	0.17	9.48
<i>Pseudomonas</i> sp. SWP-4	39.85	43.48	0.55	0.53	4.65	0.2	0.62	10.12

**Fig. 11** SEM images of the carbon steel surfaces after corrosion products were removed: (a), (c) and (e) (sterile medium); (b), (d) and (f) (medium with bacteria).

surfaces with compacted biofilm. However, the corrosion cracks were not as serious as the marine halophilic bacteria, *Pseudomonas* sp.<sup>15</sup> Combining the weight loss assessment and electrochemical measurements, we deduced that after 216 h, the surface of the carbon steel was covered with rhamnolipid that inhibited the corrosion of carbon steel. Thus, it was the rhamnolipid with high concentration that inhibited the corrosion with time prolonged.

### 3.5. Corrosion of carbon steel in sterile deionised water and oil-cell-free fermentation broth based on weight loss method

The corrosion rates during the corrosion process for 672 h immersed in the sterile deionised water and the fermentation broth containing rhamnolipid of  $2.87 \text{ g L}^{-1}$  secreted by *Pseudomonas* sp. SWP-4 were presented in Fig. 12. The corrosion rates  $0.0059 \text{ mm per year}$  of the steel coupons exposed in the fermentation broth were lower than that in the sterile deionised



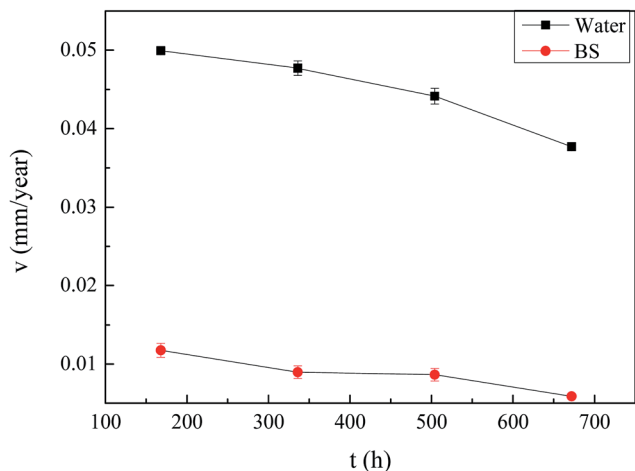


Fig. 12 Time dependence of corrosion rate changes of carbon steel immersed in sterile deionised water and the fermentation broth.

Table 6 Tafel analysis of polarization curves of the carbon steel in the deionized sterile water (DI water) and in the oil-cell-free fermentation broth

	$E_{\text{OCP}}$ (V vs. Ag/AgCl)	$i_{\text{corr}}/$ $\mu\text{A}$	$I_{\text{corr}}/$ $\mu\text{A cm}^{-2}$	$\beta_{\text{a}}/$ $\text{mV}^{-1}$	$\beta_{\text{c}}/$ $\text{mV}^{-1}$
DI water	−0.461	2.62	2.62	5.049	4.871
Fermentation broth	−0.891	2.59	2.59	3.401	8.838

water 0.0377 mm per year. It obviously showed the fermentation broth itself didn't increase corrosion rate. The result agreed with T. Meylheuc, who proved that the adsorption of rhamnolipid produced by *Pseudomonas fluorescens* inhibited the AISI 304 corrosion against the chloride diffusion.<sup>24</sup> This indicated the efficiency of the biosurfactant, rhamnolipid, which acted as

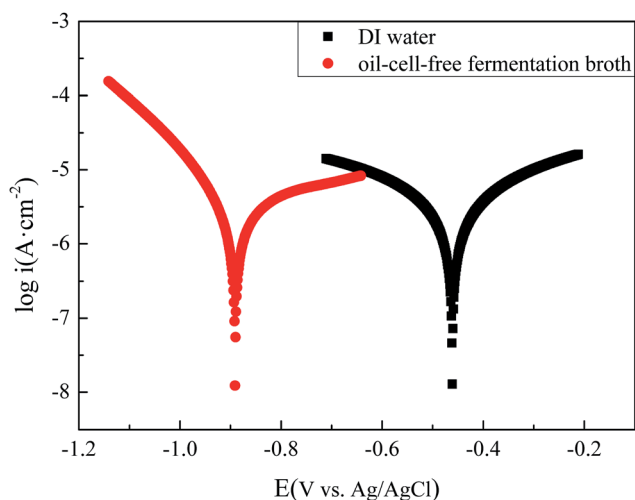


Fig. 13 Tafel plots of the carbon steel specimens in the deionized sterile water (DI water) and in the oil-cell-free fermentation broth.

a quickly-appearing barrier to the oxide, leading to the decrease of corrosion rate.

### 3.6. Corrosion of carbon steel in sterile deionised water and oil-cell-free fermentation broth based on electrochemical measures

Fig. 13 shows the polarization curves of the carbon steel respectively immersed in deionized sterile water and in the oil-cell-free fermentation broth. The data of the electrochemical corrosion parameters are analyzed with the extrapolation of the polarization and listed in Table 6. The  $i_{\text{corr}}$  ( $2.59 \mu\text{A cm}^{-2}$ ) reflected that the corrosion of carbon steel immersed in the oil-cell-free fermentation broth, which was smaller than that ( $2.62 \mu\text{A cm}^{-2}$ ) immersed in the deionized sterile water. The consequence was in agreement with weight loss result, and the corrosion rates in the fermentation broth were lower than that in the sterile deionised water which indicated that the electrochemical corrosion of oil-cell-free fermentation broth was so mild.

### 3.7. Corrosion of carbon steel in sterile deionised water and oil-cell-free fermentation broth based on SEM micrographs

As shown on the SEM observations (Fig. 14), the carbon steel immersed in the oil-cell-free fermentation broth almost remained intact, while pits had a low diameter and grew in depth the surfaces immersed in sterile deionised water. For samples conditioned by the biosurfactant, the protective oxide layer did not have time to develop because the adsorption of the biosurfactant occurred very quickly. When the sample was immersed in sterile deionised water without the biosurfactant, the oxide layer was more compact, and the number of defects increased, as shown in Fig. 14(a, c and e) which led to a higher density of pits. At these conditions the corrosion propagated much easily on the surface.

### 3.8. Antibacterial effects of oil-cell-free fermentation broth

The results about inhibitory activities of the oil-cell-free fermentation broth against 2 reference harmful bacteria in oil field: SRB and TGB were shown in Table 7. After 24 h incubation, it was obviously seen that oil-cell-free fermentation broth containing  $96 \mu\text{g mL}^{-1}$  rhamnolipid apparently manifested a good antibacterial capability on the SRB and the TGB. The results showed agreement with that Haifarajollah *et al.* who had reported rhamnolipid adsorbing on a plasma treated polypropylene surface showed appropriate antimicrobial property against the bacteria, *i.e.* *S.aureus*, *B. subtilis* and *K. pneumonia*, in food and pharmaceutical industries.<sup>31</sup>

Corrosion never stops but its scale and severity could be reduced. One of the best known methods for protection against corrosion is to use biocide. Biocide has been proved that could control the corrosion of different metals and alloys. In the light of that, it's necessary for us to study biocide/inhibitor effect on SRB on carbon steel corrosion.

This study may provide theoretical information for the application of oil-cell-free fermentation broth inhibiting carbon steel corrosion in oil industrial environment. Moreover, rhamnolipid, a biosurfactant which is biodegradable, also could inhibit the increasing of SRB. The results presented here





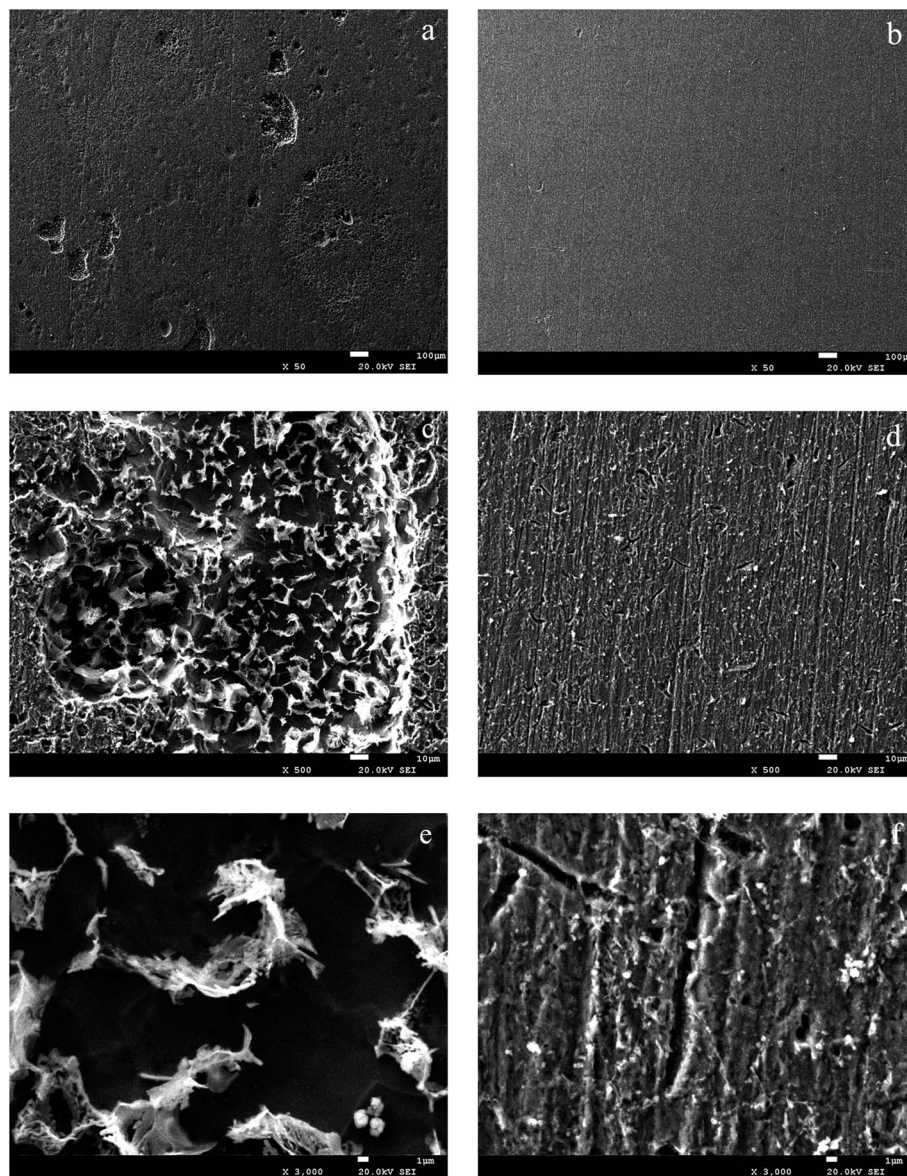


Fig. 14 SEM images of the carbon steel surfaces after corrosion products were removed: (a), (c) and (e) (sterile deionised water); (b), (d) and (f) (oil-cell-free fermentation broth).

Table 7 The results of antibacterial property test

Bacteria type	0 $\mu\text{g mL}^{-1}$	32 $\mu\text{g mL}^{-1}$	96 $\mu\text{g mL}^{-1}$	160 $\mu\text{g mL}^{-1}$	320 $\mu\text{g mL}^{-1}$	640 $\mu\text{g mL}^{-1}$
SRB	2750	110	0.6	25	70	275
TGB	42	32	22	43	37	44

could provide useful information for MIC, and more experiments should be performed to find out a useful and environmental biocide/inhibitor against corrosion.

## 4. Conclusions

Firstly, *Pseudomonas* sp. SWP-4 caused a weak corrosion behavior on the carbon steel with a corrosion rate of 0.0137 mm per year.

The approaching to neutral pH of the medium may contribute to the passive film, resist to the aggressiveness of the medium and then the surface kept in a good protection. EDS approved that *Pseudomonas* sp. SWP-4 excluded oxygen *via* respiration compared to corrosion products of carbon steels immersed in the MSM. Electrochemical results (Tafel plots and EIS measurements) showed that during the exponential phase of bacteria growth, *Pseudomonas* sp. SWP-4 consumed the dissolved oxygen and adsorbed mineral salts and the changeable characteristic of medium accelerated the corrosion rate of carbon steel. From the stationary phase, electrochemical results indicated that fermentation broth of *Pseudomonas* sp. SWP-4 appeared to without the electrochemical corrosive property. Secondly, it proved that oil-cell-free fermentation broth of *Pseudomonas* sp. SWP-4 could inhibit the corrosion, and the corrosion rate with



the bacterium was 0.0059 mm per year while that in sterile water was 0.0377 mm per year, which was in agreement with the theory that biosurfactant could act as a barrier to oxygen. Furthermore, SEM showed a patchy distribution over the carbon steel surface. While the oil-cell-free fermentation broth inhibited the corrosion activity of carbon steel and inhibited the increasing of SRB. This could be a good suggestion to make *Pseudomonas* sp. SWP-4 used widely in oil fields.

## Acknowledgements

This work was financially supported by the Open Projects of Key Laboratory of Oil & Gas Applied Chemistry of Sichuan Province, Southwest Petroleum University, PR China (YQKF201406). Open Projects of Key Laboratory of Development and Application of Rural Renewable Energy, Ministry of Agriculture, PR China. (2015004)

## References

- 1 E. J. Gudiña, J. F. Pereira, L. R. Rodrigues, J. A. Coutinho and J. A. Teixeira, *Int. Biodeterior. Biodegrad.*, 2012, **68**, 56–64.
- 2 N. Parmar, A. Singh and O. Ward, *Biotech in Enhanced Petroleum Oil Recovery*, Springer Group Publisher, 2014, pp. 239–245.
- 3 W. J. Xia, Z. B. Luo, H. P. Dong, L. Yu, Q. F. Cui and Y. Q. Bi, *Appl. Biochem. Biotechnol.*, 2012, **166**, 1148–1166.
- 4 N. Khondee, S. Tathong, O. Pinyakong, R. Müller, S. Soonglerdsongpha, C. Ruangchainikom, C. Tongcumpou and E. Luepromchai, *Biochem. Eng. J.*, 2015, **93**, 47–54.
- 5 C. Zou, M. Wang, Y. Xing, G. Lan, T. Ge, X. Yan and T. Gu, *Biochem. Eng. J.*, 2014, **90**, 49–58.
- 6 R. Pasumarthi, S. Chandrasekaran and S. Mutnuri, *Mar. Pollut. Bull.*, 2013, **76**, 276–282.
- 7 X. Zhang, D. Xu, C. Zhu, T. Lundaa and K. E. Scherr, *Chem. Eng. J.*, 2012, **209**, 138–146.
- 8 M. J. Johnson and F. Jarvis, *J. Am. Chem. Soc.*, 1949, **71**, 4124–4126.
- 9 G. Lan, Q. Fan, Y. Liu, C. Chen, G. Li, Y. Liu and X. Yin, *Biochem. Eng. J.*, 2015, **101**, 44–54.
- 10 G. Lan, Q. Fan, Y. Liu, Y. Liu, Y. Liu, X. Yin and M. Luo, *Biochem. Eng. J.*, 2015, **103**, 219–226.
- 11 D. C. White, M. J. Franklin and H. S. Isaacs, *Corros. Sci.*, 1991, **32**, 945–952.
- 12 E. Hamzah, M. F. Hussain, Z. Ibrahim and A. Abolahi, *Arabian J. Sci. Eng.*, 2014, **39**, 6863–6870.
- 13 P. Esparza, J. Morales, S. González, R. Salvarezza and M. P. Arévalo, *Biofouling*, 1993, **34**, 129–139.
- 14 M. Moradi, Z. Song, L. Yang, J. Jiang and J. He, *Corros. Sci.*, 2014, **84**, 103–112.
- 15 S. Kjelleberg, A. Pedersen and M. Hermansson, *J. Microbiol. Methods*, 1988, **8**, 191–198.
- 16 M. Vazquez, J. P. Busalmen and S. R. de Sanchez, *Electrochim. Acta*, 2002, **47**, 1857–1865.
- 17 I. B. Beech, V. Zinkevich, L. Hanjansit, R. Gubner and R. Avci, *Biofouling*, 2000, **15**, 3–12.
- 18 L. Hanjansit, I. B. Beech, M. Kalaji, A. L. Neal and V. Zinkevich, *Microbiology*, 1999, **145**, 1491–1497.
- 19 C. C. Gaylarde and I. B. Beech, *Int. Biodeterior.*, 1991, **27**, 95–107.
- 20 I. B. Beech, R. Gubner, V. Zinkevich, L. Hanjansit and R. Avci, *Biofouling*, 2000, **16**, 93–104.
- 21 N. O. San, H. Nazir and G. Donmez, *Corros. Sci.*, 2014, **79**, 177–183.
- 22 L. C. Xu, K. Y. Chan and H. H. P. Fang, *Environ. Sci. Technol.*, 2002, **36**, 1720–1727.
- 23 S. J. Yuan, A. M. F. Choong and S. O. Pehkonen, *Corros. Sci.*, 2007, **49**, 4352–4385.
- 24 C. Dagbert, T. Meylheuc and M. N. Bellon-Fontaine, *Electrochim. Acta*, 2006, **51**, 5221–5227.
- 25 T. Meylheuc, C. Dagbert and M. N. Bellon-Fontaine, *Electrochim. Acta*, 2008, **54**, 35–40.
- 26 F. Liu, J. Zhang, C. Sun, Z. Yu and B. Hou, *Corros. Sci.*, 2014, **83**, 375–381.
- 27 P. J. Antony, R. K. S. Raman, R. Raman and P. Kumar, *Corros. Sci.*, 2010, **52**, 1404–1412.
- 28 D. Cetin and M. L. Aksu, *Corros. Sci.*, 2009, **51**, 1584–1588.
- 29 B. W. A. Sherar, I. M. Power, P. G. Keech, S. Mitlin and G. Southam, *Corros. Sci.*, 2011, **53**, 955–960.
- 30 L. Magalhães and M. Nitschke, *Food Control*, 2013, **29**, 138–142.
- 31 H. Hajfarajollah, S. Mehvari, M. Habibian, B. Mokhtarani and K. A. Noghabi, *RSC Adv.*, 2015, **5**, 33089–33097.
- 32 P. Bharali, J. P. Saikia, A. Ray and B. K. Konwar, *Colloids Surf.*, 2013, **103**, 502–509.
- 33 T. Meylheuc, M. Renault and M. N. Bellon-Fontaine, *Int. J. Food Microbiol.*, 2006, **109**, 71–78.
- 34 T. Lotfabad, F. Shahcheraghi and F. Shooraj, *Jundishapur J. Microbiol.*, 2012, **6**, 29–35.
- 35 M. Dubois, K. A. Gilles, J. K. Hamilton, P. A. Rebers and F. Smith, *Anal. Chem.*, 1956, **28**, 350–356.
- 36 A. Leyva, A. Quintana, M. Sanchez, E. N. Rodriguez, J. Cremata and J. C. Sanchez, *Biologicals*, 2008, **36**, 134–141.
- 37 M. Benincasa, J. Contiero, M. A. Manresa and I. O. Moraes, *J. Food Eng.*, 2002, **54**, 283–288.
- 38 D. Cetin, S. Bilgiç, S. Dönmez and G. Dönmez, *Mater. Corros.*, 2007, **58**, 841–847.
- 39 J. T. Walker and C. W. Keevil, *Int. Biodeterior. Biodegrad.*, 1994, **33**, 223–236.
- 40 S. O. Pehkonen, X. H. Zhang, N. Kocherginsky and G. A. Ellis, *Corros. Sci.*, 2002, **44**, 2507–2528.
- 41 W. K. Teo, Y. Feng, K. S. Siow and A. K. Hsieh, *Corros. Sci.*, 1996, **38**, 387–395.
- 42 H. A. Videla, *Manual de Biocorrosion*, CRC Press, 1996.
- 43 S. Bayoudh, A. Othmane, L. Ponsonnet and H. Ben Ouada, *Colloids Surf. A*, 2008, **318**, 291–300.
- 44 Y. Yin, S. Cheng, S. Chen, J. Tian, T. Liu and X. Chang, *Mater. Sci. Eng.*, 2009, **29**, 756–760.

